

# MATERIAL PROPERTIES OF OSTEOCHONDRAL CONSTRUCTS AND BIPHASIC FINITE ELEMENT MODELS OF DYNAMIC LOADING FOR ARTICULAR CARTILAGE TISSUE ENGINEERING

Eric G. Lima\*, Robert L. Mauck\*, Seonghun Park<sup>†</sup>, Selom Gasinu\*, Kenneth W. Ng\*, Clark T. Hung\*, Gerard A. Ateshian\*\*

\*Department of Biomedical Engineering,  
Columbia University, New York, NY

<sup>†</sup>Department of Mechanical Engineering,  
Columbia University, New York, NY

## INTRODUCTION

The poor intrinsic healing capacity and a lack of effective clinical repair strategies for articular cartilage has generated great interest in the engineering of articular cartilage replacement tissues (e.g., [1,2]). Agarose hydrogels provide a 3D environment conducive to such tissue-engineering endeavors, as it maintains chondrocyte phenotype and allows for the development of a functional extracellular matrix [3]. With time in culture, chondrocyte-seeded agarose hydrogels increase in tissue properties and respond to short-term applied deformational loading in a manner similar to native tissue [4]. Furthermore, long-term deformational loading of these constructs increases tissue properties of constructs compared to free swelling controls [5,6]. As these engineered constructs approach the mechanical and biochemical properties of the native tissue, significant new challenges have become apparent. In particular, integration of these constructs into the damaged articular surface remains a difficult problem. One possible solution to this may be the development of engineered osteochondral constructs [7,8] similar to those used for autologous transplantation [9]. In previous studies, osteochondral constructs composed of a cell-seeded agarose layer integrated with a trabecular subchondral bony layer were shown to increase in biochemical and material properties with time in free swelling culture [10]. With the intent of applying dynamic deformational loading to these constructs, the goals of the current study were (1) to ascertain how the material properties of agarose osteochondral constructs might differ from those of agarose disks depending on the apparent density of the underlying bony substrate, (2) to determine the local deformational gradients within the osteochondral constructs, and (3) to develop biphasic finite element models to predict the mechanical stimuli that may arise with dynamic deformational loading of these osteochondral constructs.

## MATERIALS AND METHODS

**Osteochondral Construct Preparation:** Cylindrical trabecular bone cores, Ø 5 mm x 4 mm thick, were harvested from the epiphysis of metatarsal bones of 3 month-old calves. Cores were cut to size and cleaned of marrow with a water pick, and mass and volume measurements were taken to determine the apparent density. Cores

were grouped by density, and infused with a molten 3% (in PBS) agarose hydrogel (Type VII, Sigma) in a custom mold to produce constructs with an ~2mm gel-only region, an ~2 mm gel-bone interface region, and a ~2mm bone-only region. **Mechanical Testing:** Constructs were tested in unconfined compression (n=5) with stress relaxation tests to 10% strain (of upper gel thickness) followed by dynamic testing (with an applied displacement of 20 µm) at frequencies ranging from 0.005-1 Hz. The Young's and dynamic modulus were calculated from the measured stress and the specimen geometry. **Displacement Fields:** To obtain an axial displacement field, osteochondral constructs were cut in half and compressed using a custom compression device mounted on the stage of an inverted microscope. The initial thickness of the specimen was measured optically (1.66 µm/pixel) and a 5% tare strain was applied. After equilibrium, an image was taken, and the specimen was further compressed another 5% strain increment with a second image acquired after equilibrium. Image analysis was performed using an automated digital image correlation technique to produce an axial displacement field [11]. **Biphasic Finite Element Models:** Finite element meshes were constructed with a commercial software package to model the compression of agarose (2 mm thickness x 5 mm diameter) and osteochondral composite constructs (4 mm thickness x 5 mm diameter, with 1 mm of gel-bone region). Axisymmetric meshes contained 600 elements with eight nodes per element, with the distribution of elements biased towards the free edge. Each region was assumed homogenous, with a linear isotropic elastic solid matrix, with the gel region having  $E_V=10$  kPa,  $\nu=0.3$ ,  $k=1 \times 10^{-12}$  m<sup>4</sup>/Ns, the gel-bone region having  $E_V=1000$  MPa,  $\nu=0.3$ ,  $k=0.25 \times 10^{-12}$  m<sup>4</sup>/Ns, and the bone region having  $E_V=1000$  MPa,  $\nu=0.3$ ,  $k=1 \times 10^{-8}$  m<sup>4</sup>/Ns. A custom FEM program incorporating biphasic theory [12] was used to model the resulting mechanical forces generated as a result of both a stress relaxation test (to 10% strain) and an applied sinusoidal strain with a magnitude of 10% of the gel thickness and a frequency of 1 Hz. Results from the finite element analysis were output at equilibrium for stress relaxation testing ( $t=1000$  s) or the point of maximal deformation ( $t=0.5$  s) for dynamic deformational loading.

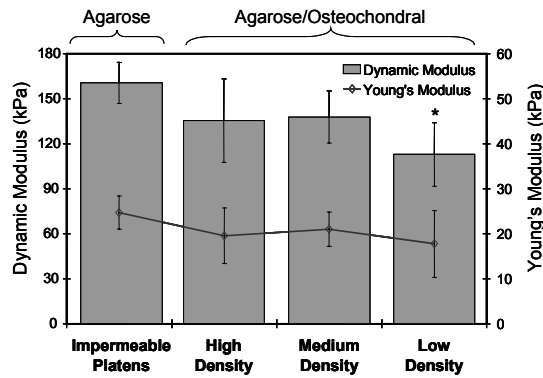


**Figure 1 – Dynamic (at 0.5 Hz) and Young's Modulus for agarose and agarose/osteocondral constructs with differing subchondral bone density (n=5).**

**RESULTS**

Bone cores were found to vary in apparent density, and were grouped into high ( $0.46 \pm 0.05$ ), medium ( $0.36 \pm 0.03$ ), and low ( $0.24 \pm 0.03$ ) density groups. Mechanical testing of osteochondral constructs revealed no statistical difference in the Young's modulus with decreasing density of the underlying trabecular bone compared to gel-alone constructs (Figure 1). However, the dynamic modulus decreased significantly ( $p < 0.05$ ) in the case of the lowest density subchondral bone osteochondral constructs compared to gel-alone constructs (Figure 1). Microscopic evaluation of the axial displacement field of osteochondral constructs in unconfined compression (Figure 2A) revealed that deformation occurred solely in the gel region (Figure 2B). A FEM simulation of stress relaxation generated a similar deformation profile at equilibrium (Figure 2C). FEM modeling of dynamic deformational loading of gel-alone or osteochondral constructs showed quantitative and qualitative differences in the magnitude and distribution of mechanical signals. In particular, fluid pressure was uniform through the thickness and radial direction in gel-alone constructs, while there was a higher, and much less uniform distribution of pressure in osteochondral constructs (Figure 3). Fluid flux was directed radially and was greatest at the edges of gel-alone constructs. In osteochondral constructs, high flows were observed at the radial edge (highest at the interface of the gel layer with the subchondral bone), with some flow through the bottom of the gel into the bone-gel region (Figure 3). Significant variation of fluid pressurization occurred in the bone-gel region as well, and was highest at the gel/bone-gel interface, and decreased to ambient levels at the bone-gel/bone interface. Radial strain in gel-alone constructs was largely homogeneous, while strains were larger in magnitude and heterogeneously distributed in osteochondral constructs (Figure 4).

**DISCUSSION**

Osteochondral constructs with low-density bone were found to have a decreased dynamic modulus compared to gel-alone cylindrical constructs. This finding may be explained by the increased area for fluid flow (i.e., both radially and axially through the subchondral

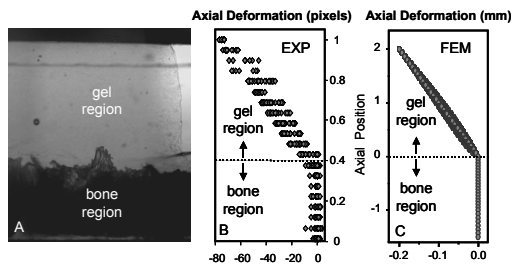


**Figure 2 – Deformation field of osteochondral construct (A) measured (B) and predicted (C) with FEM model.**

bone) in osteochondral constructs compared to gel-alone constructs. Stress-relaxation of agarose osteochondral constructs in unconfined compression resulted in deformation occurring only in the softer gel region. Biphasic FEM models predicted that dynamic deformational loading of osteochondral constructs would create pressure, flow, and radial strains that are quantitatively and qualitatively different from those in gel-alone constructs. In particular, the gel region experiences variations in pressure, a dynamic axial normal strain, and a radial normal strain that is highest at the surface and minimal at the gel-bone interface. The gel-bone region experiences a fluctuating fluid pressure with no deformation. These findings highlight the differences in mechanical environment that would be seen by cells seeded in the various regions of an osteochondral construct. These differing load-induced signals will likely alter the developing mechanical properties and matrix distribution in osteochondral constructs compared to gel-alone controls, and may be harnessed to encourage the development of tissue inhomogeneity (tensile properties in the surface region and subchondral plate formation at the gel-bone interface) in engineered osteochondral constructs.

**ACKNOWLEDGEMENTS**

This study was supported by the NIH [R01 AR46568 and R01 AR46532] and a graduate fellowship from the Whitaker Foundation.

**REFERENCES**

[1] Freed LE, et al., 1997, *Proc Natl Acad Sci USA*, 94:13885-13890. [2] Vunjak-Novakovic G, et al., 1999, *J Orthop Res*, 17:130-138. [3] Benya and Shaffer, 1982, *Cell*, 30:215-224. [4] Buschmann MD, et al., 1995, *J Cell Sci*, 108:1497-1508. [5] Mauck RL, et al., 2002, *Ann Biomed Eng*, 30:1046-1056. [6] Mauck RL, et al., 2000, *J Biomech Eng*, 122:252-260. [7] Sherwood JK, et al., 2002, *Biomaterials*, 23:4739-4751. [8] LeRoux MA, et al., 2002, *Trans Orthop Res Soc*, 27:469. [9] Hangody L, et al., 1996, *7th Congress of the ESSK*, pp. 99-100. [10] Takai E, et al., 2003, *Trans ORS*, accepted. [11] Wang CCB, et al., 2002, *J Biomech Eng*, submitted. [12] Mow VC, et al., 1980, *J Biomech Eng*, 102: 73-84.

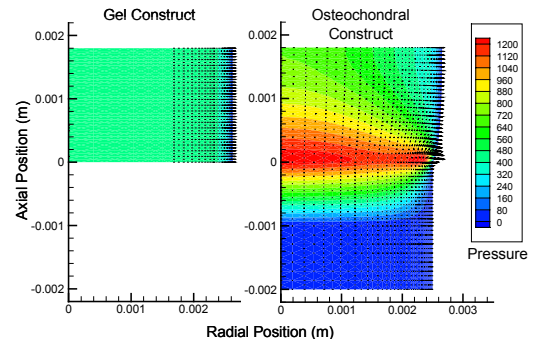


**Figure 3 –Pressure (Pa) and fluid flux (arrows) in dynamically loaded agarose (left) or osteochondral constructs (right).**

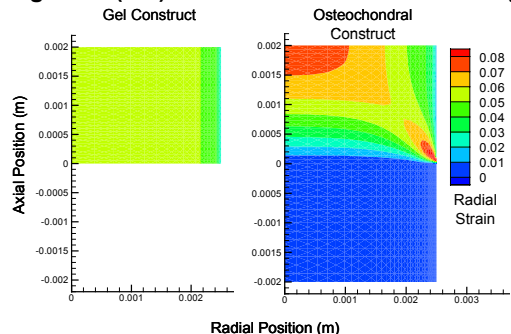


**Figure 4 – Radial strain in dynamically loaded agarose (left) and osteochondral (right) constructs.**